Combustion and Flame 260 (2024) 113202

Contents lists available at ScienceDirect

Combustion and Flame

journal homepage: www.sciencedirect.com/journal/combustion-and-flame

Coupling chemical lumping to data-driven optimization for the kinetic modeling of dimethoxymethane (DMM) combustion

Alessandro Pegurri, Timoteo Dinelli, Luna Pratali Maffei, Tiziano Faravelli, Alessandro Stagni *

Department of Chemistry, Materials, and Chemical Engineering "G. Natta", Politecnico di Milano, Milano, 20133, Italy

ARTICLE INFO

Keywords:
Kinetic modeling
Chemical lumping
Numerical optimization
Dimethoxymethane
DMM
Oxymethylene ethers

ABSTRACT

The kinetic mechanisms describing the combustion of longer-chain fuels often have limited applicability due to the high number of species involved in their oxidation and decomposition paths. This work proposes a combined methodology for developing compact but accurate kinetic mechanisms of these fuels and applies it to dimethoxymethane (DMM), or oxymethylene ether 1 (OME_1). An automatic chemical lumping procedure, performed by grouping structural isomers into pseudospecies, was proposed and applied to a detailed kinetic model of DMM pyrolysis and oxidation, built from state-of-the-art kinetic sub-models. Such a methodology proved particularly efficient in delivering a compact kinetic mechanism, requiring only 11 species instead of 35 to describe DMM sub-chemistry. The obtained lumped kinetic model was then improved through a data-driven optimization procedure, targeting data artificially generated by the reference detailed mechanism. The optimization was performed on the physically-constrained parameters of the modified-Arrhenius rate constants of the controlling reaction steps, identified via local sensitivity analyses. The dissimilarities between the predictions of the detailed and lumped models were minimized using a Curve Matching objective function for a comprehensive and quantitative characterization. Above all, the optimized mechanism was found to behave comparably to the starting detailed one, throughout most of the operating space and target properties (ignition delay times in shock tubes, laminar flame speeds, and speciations in stirred and flow reactors). The successful application of the proposed methodology to the DMM chemistry paves the way for its extensive use in the kinetic modeling of longer OMEs as well as heavier fuels, for which the computational advantages are expected to be even higher.

1. Introduction

Achieving a long-term carbon-neutral economy requires an eclectic strategy, involving the implementation of parallel measures to gradually decrease the dependence on fossil fuels. The transportation sector is the second largest emitter of greenhouse gases after the energy industries, and largely contributes to the global warming phenomenon [1]. To address the issue, the European Union has recently approved a package of laws that aims to reduce emissions by 55% by 2030 compared to 1990 levels and achieve climate neutrality by 2050 [2]. The package includes a specific section for the transportation sector, which mandates that all new cars entering the market from 2035 should be zero-emission vehicles. According to this, electric vehicles might look like the first-line choice, but as long as electricity is mostly produced by fossil fuels, they do not tackle the issue of greenhouse-gas emissions. Additionally, an important limitation of carbon-free, renewable sources like wind or solar energy is their intermittent availability, such that storing excess energy and releasing it "on demand" is one of the most debated issues of the current energy transition. For this reason, the production and use of synthetic fuels, or e-fuels, to accumulate the energy produced from renewable sources has become a major research line [3].

In this scenario, oxymethylene ethers (OME_n) have recently been identified as a suitable candidate to progressively replace traditional fuels in diesel engines [4]. This is due to multiple reasons: (i) they rely on an established catalytic synthesis [5–8]; (ii) their physico-chemical properties are comparable to those of diesel fuels, especially in terms of miscibility and ignition propensity [9]; (iii) their oxygenated nature ensures a noticeable reduction in soot and particulate matter formation, as highlighted by several experimental [10–14] and numerical [15–20] studies.

Dimethoxymethane (DMM, i.e. OME_1) is the shortest OME after dimethyl ether (DME, i.e. OME_0), therefore knowing its chemistry is essential to model the reactivity of longer-chain OMEs. As a result, the interest in the chemical kinetics of DMM rapidly increased over the past

* Corresponding author.
E-mail address: alessandro.stagni@polimi.it (A. Stagni).

https://doi.org/10.1016/j.combustflame.2023.113202
Received 29 June 2023; Received in revised form 15 November 2023; Accepted 17 November 2023
Available online 30 November 2023

Nomenclature

Acronyms

BF	Branching fraction
DME	Dimethyl ether
DMM	Dimethoxymethane
IDT	Ignition delay time
JSR	Jet stirred reactor
LFS	Laminar flame speed
MEL	Master Equation-based lumping
OME	Oxymethylene ether
PES	Potential Energy Surface
PFR	Plug flow reactor
SM	Supplementary Material

Greek Symbols

λ	Air-fuel equivalence ratio [-]
Φ	Fuel-air equivalence ratio [-]

Roman Symbols

k	Kinetic constant [mol, cm, s]
P	Pressure [Pa]
T	Temperature [K]
t	Time [s]
X	Isomer branching fraction [-]
x	Mole fraction [-]

years; available studies focus on both theoretical calculations for the rate constants estimation [21–23] and their subsequent implementation in kinetic models [24–27].

The major drawback of a detailed kinetic mechanism for DMM combustion is the resulting large number of species and reactions, which increase even further for longer-chain OMEs. Such kinetic mechanisms are therefore hardly applicable to large-scale simulations, and preliminary reduction techniques need to be adopted to perform computational fluid dynamics simulations [28].

On the other hand, the hierarchical nature of OMEs and their regular structure make them particularly suitable for a lumped formulation of their kinetics. Previous literature studies [29–32] showed the potential of the lumping approach in developing compact, low-to-high-temperature mechanisms of long-chain fuels, without a significant loss in the accuracy of the predictions of ignition propensity and speciations. Moreover, such methodologies can be combined with a downstream optimization of the lumped kinetic parameters for an improved agreement with the detailed model.

In this work, an integrated methodology coupling a novel chemical lumping procedure and a subsequent mechanism optimization is presented. In particular, an automatic lumping methodology, performed by grouping structural isomers into the same pseudospecies, is applied to a detailed kinetic model. The rate parameters are then refined by adopting a data-driven optimization methodology, based on artificial data generation through the reference detailed mechanism, to minimize the differences from the original model. Both lumping and optimization methodologies are implemented into two separate open-source, freely available tools.

As a case study, the kinetic model of DMM pyrolysis and oxidation is developed from a state-of-the-art sub-model available in the literature [22]. Its compact size allows a thorough analysis of the effects of the methodology on the performance of the reduced mechanism. This is benchmarked against the detailed one, and the advantages and potential improvements of the proposed approach are summarized. To confirm the reproducibility of the methodology, a second reduction was performed on the kinetics of OME_2, whose validation is presented in the Supplementary Materials (SM) for the sake of compactness.

2. Methodology

2.1. Detailed kinetic model

The detailed kinetic model describing the pyrolysis and oxidation of DMM was built up through a hierarchical and modular procedure, starting from the CRECK kinetic modeling framework [33]. Among CRECK subsets, the C_0-C_3 mechanism (adopted and updated from previous works [34–37]) was used as a basis for OMEs chemistry.

Ethers' chemistry was taken into account starting from the DME sub-mechanism by Burke et al. [38]. Similarly, the DMM sub-mechanism was integrated from the work of Jacobs et al. [22]. Both involve pressure-dependent estimates of low-temperature chemistry and were validated in a wide range of operating conditions. Thermodynamic properties were updated according to the database of Burcat and Ruscic [39].

The detailed kinetic mechanism obtained in such a way includes 161 species and 2283 reactions and was adopted as a starting point to develop the lumped mechanism. It is available in CHEMKIN format as SM of this work.

2.2. Chemical lumping

The DMM lumped kinetics was derived from the detailed one, by extending a master equation-based lumping methodology (MEL, available at https://github.com/lpratalimaffei/MEL), initially conceived for processing the output of multi-well master equation simulations [40], thus simplifying their complexity. For the first time, such methodology was extended to include reaction pathways from multiple potential energy surfaces (PESs) that interact significantly. The result is an automatic approach that calculates lumped rates requiring minimal external input. The approach also automatically identifies species that do not accumulate in kinetic simulations and can therefore be removed from the reaction pathways in the lumping step rather than in a subsequent skeletal reduction. The lumping procedure was performed by grouping similar species into pseudospecies. Structural isomerism was the chosen grouping criterion so that the same functional groups were retained in each pseudospecies. The choice of the pseudospecies and the respective composition is the only lumping step that requires the user's knowledge of the mechanism. Due to the fictitious nature of pseudospecies, all reactions were written as irreversible.

The composition of each pseudospecies was evaluated as a function of temperature and pressure via 0D isothermal and isobaric simulations, performed with the detailed mechanism in a temperature range of 500–2000 K. Such a procedure had already been successfully adopted in previous works to perform species-targeted mechanism reduction [41], where accuracy was shown to be retained, too, in 1D flames for the same species. Logarithmically spaced pressures in the range of 0.001–500 atm were considered to cover the whole range of pressure-dependent reactions (in PLOG format) of the detailed mechanism [22]. Lean conditions ($\Phi = 0.5$) were chosen to emphasize low-temperature oxidation kinetics, where the lumped pseudospecies play a major role. Nevertheless, the influence of Φ on the pseudospecies' composition was verified a posteriori to be minimal.

The average, temperature-dependent branching fractions (BFs) of each pseudospecies were thus adopted for the evaluation of the lumped rates parameters. Branching fractions BF_i of each ith isomer for a given pseudospecies were calculated as in Eq. (1):

$$BF_i = \frac{\int_0^{t_{max}} X_i(t)dt}{t_{max}} \tag{1}$$

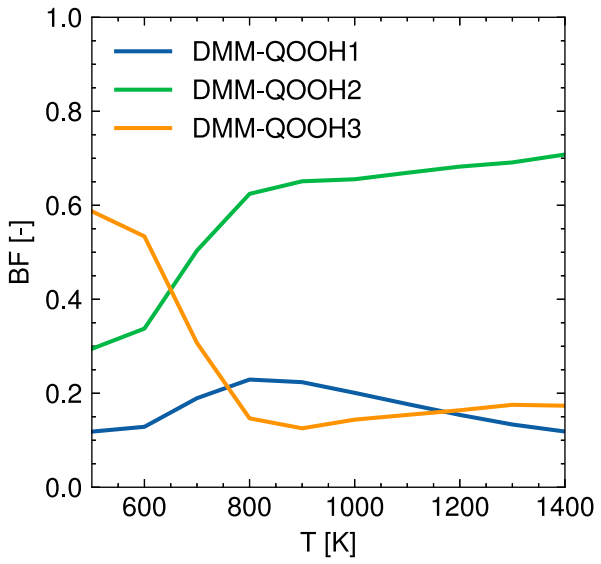

Fig. 1. Branching fractions of DMM-QOOH isomers at atmospheric pressure, as a function of the temperature.

where X_i is the ith isomer fraction with respect to the total isomers pool, defined as in Eq. (2):

$$X_i(t) = \frac{x_i(t)}{\sum_i x_i(t)} \tag{2}$$

where x_i is the mole fraction of the ith isomer. In Eq. (1), t_{max} is the time, in the 0D simulation, when the total isomers mole fraction reaches its maximum value. The choice to ignore the successive consumption phase ensures smoother BF profiles with respect to the temperature. An example of isomer pool composition for the lumped hydroperoxy alkyl radical (DMM-$\dot{Q}$OOH) at atmospheric pressure is shown in Fig. 1.

The evaluation process of the BF was specifically developed for this methodology and differs majorly from the one used in typical applications of MEL. In fact, contrarily to [40], the strong non-equilibrium interactions between lumped groups of species prevent the use of simple equilibrium/steady state compositions for the lumped species obtained from the reactivity of single PESs. One of the advantages of this approach is its generality for all lumped species. Similar approaches from the literature (e.g., [30]) treat high- and low-temperature isomers differently to account for their different intrinsic reactivity, for example, distinguishing between primary and secondary radicals. This not only increases the total number of species but also requires a critical evaluation of the kinetics from the user.

In this work, the thermodynamic and transport properties of the most abundant isomer in each pool were selected for the corresponding pseudospecies, as widely accepted in the literature [30,32,42]. Moreover, since all lumped species are isomers, both their thermodynamic and transport properties are similar among the same pool and the committed error is negligible.

The rate parameters for the lumped reactions were automatically evaluated by MEL as in Eqs. (3) and (4), where R stands for reactants and Pr for products, subscript L indicates lumped species and subscript i denotes the ith isomer of the pseudospecies. Specifically:

- Rate constants of reactions without pseudospecies as reactants (e.g., H-abstractions from the fuel) were obtained by summing the respective detailed constants, as in Eq. (3). These reactions involve pseudospecies only as products, therefore their estimated rates are accurate and do not depend on BFs;

$$k_{R\rightarrow Pr_L}(T) = \sum_i k_{R\rightarrow Pr_i}(T) \tag{3}$$

- Reactions with reacting pseudospecies were lumped by averaging their detailed rates weighted on the BFs of the lumped species, as in Eq. (4). The products may be lumped as well, but it does not influence the reaction rate evaluation.

$$k_{R_L\rightarrow Pr}(T) = \sum_i BF_i(T) k_{R_i\rightarrow Pr}(T) \tag{4}$$

The reaction rates thus obtained were subsequently fitted in a modified-Arrhenius format. Differently from other literature approaches (e.g., Pepiot-Desjardins et al. [32]) where lumped rate constants are derived simultaneously as a function of a set of space variables (T, P, simulation profiles) and therefore depend on this set, in this work the problems of finding pseudospecies compositions and lumped rate constants are decoupled. The derivation of lumped rate constants is performed within each separate PES, thus substantially reducing both computational cost and the variability of the lumped rate constants.

The lumped kinetic mechanism can be found in the SM, as well as the complete species nomenclature.

2.3. Artificial data generation and data-driven optimization

The lumped mechanism underwent an optimization procedure for an enhanced agreement with the detailed reference model. To this purpose, the methodology proposed by Bertolino et al. [43] was implemented, and applied to a lumped mechanism for the first time using the `OptiSMOKE++` toolbox [44] (available at https://github.com/burn-research/OptiSMOKE_toolbox). This approach exploits an evolutionary algorithm to optimize the modified-Arrhenius parameters of the rate constants of the most impactful reactions, previously identified via sensitivity analyses. One of its major strengths lies in the capability to perform a physically consistent optimization of pressure-dependent rate constants (formulated in PLOG format in this work) throughout the whole temperature and pressure domain. This means that the original dependency on the pressure is maintained throughout the optimization. This is ensured by optimizing a set of three parameters for each rate in PLOG format from which all the others are scaled, instead of separately optimizing all the parameters for each pressure. An example is reported in Fig. 2 for the reaction DMM-R+O_2⇒DMM-RO_2 (addition of oxygen to the alkyl radical), where it is highlighted that the rate constant has been consistently optimized, i.e., it has been reduced by a factor ~2.5 for each pressure.

All three modified-Arrhenius parameters were chosen to be optimized for each reaction. In `OptiSMOKE++`, it is possible to specify which parameters to optimize for each rate, and the algorithm bounds each parameter according to the uncertainty factors provided for the rate [43,44]. The optimization methodology varied according to the type of reaction as follows:

- Reactions without reacting pseudospecies (e.g., H-abstractions from the fuel) were not optimized, as their lumped rate constant is independent from BFs (cf. Eq. (3));
- Rate constants lumped by averaging their detailed constants, as in Eq. (4), were physically constrained for each temperature between the highest and the lowest detailed rate constants (Fig. 3.a);
- Rate constants derived as a fraction of a single detailed reaction (e.g., decompositions of single isomers) were bounded between the detailed constant and a lower boundary chosen to be symmetric in a logarithmic scale (Fig. 3.b). This results in the nominal rate constant being always in the middle between the upper and lower limits in a logarithmic scale.

The possible loss of physical meaning in unbounded optimizations is a problem that is not addressed in previous approaches (e.g., [32]) where optimization boundaries do not seem to be specified. An unbounded optimization, or one with physically inconsistent boundaries,

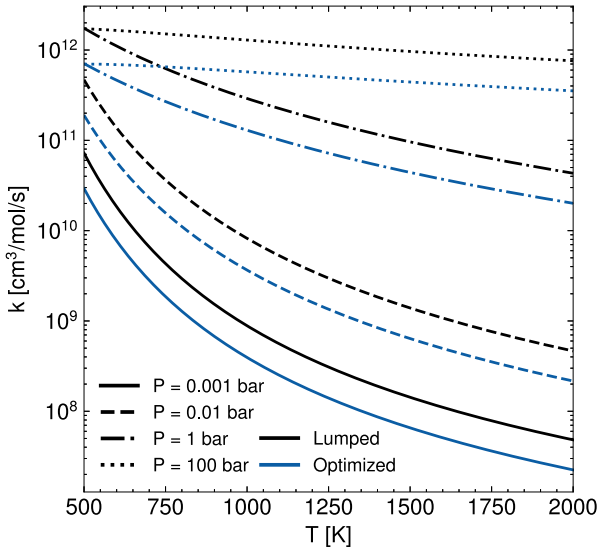

Fig. 2. DMM-R+O_2⇒DMM-RO_2 lumped rate constants before (black line) and after (blue line) optimization at 0.001–100 bar. The optimization algorithm ensures that the PLOG consistency is maintained by modifying the constant of the same quantity for each pressure.

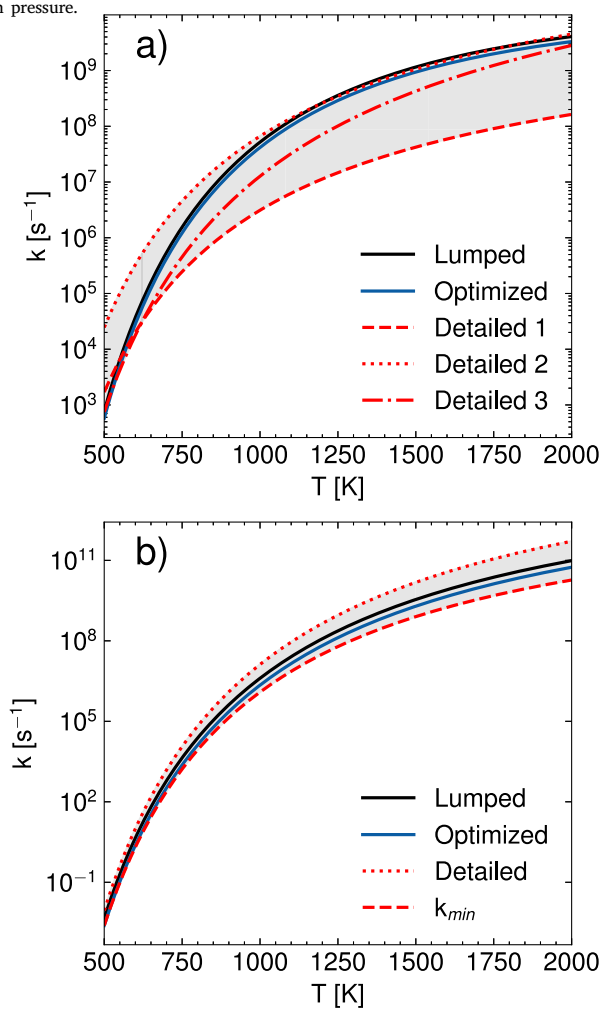

Fig. 3. Lumped rate constants of DMM-RO_2⇒DMM-QOOH (a) and DMM-OQOOH decomposition (b), before (black line) and after (blue line) optimization. The two reactions exemplify the optimization boundaries adopted for rate constants derived from multiple detailed rate constants (a) and from a single one (b). For case (a), the three detailed reactions are DMM-RO_2-1⇒DMM-QOOH-1 (red dashed line), DMM-RO_2-1⇒DMM-QOOH-2 (red dotted line), and DMM-RO_2-2⇒DMM-QOOH-3 (red dash-dotted line), respectively, while for case (b) the detailed reaction is DMM-OQOOH-3⇒CH_3O+CO_2+CH_2O+OH (red dotted line).

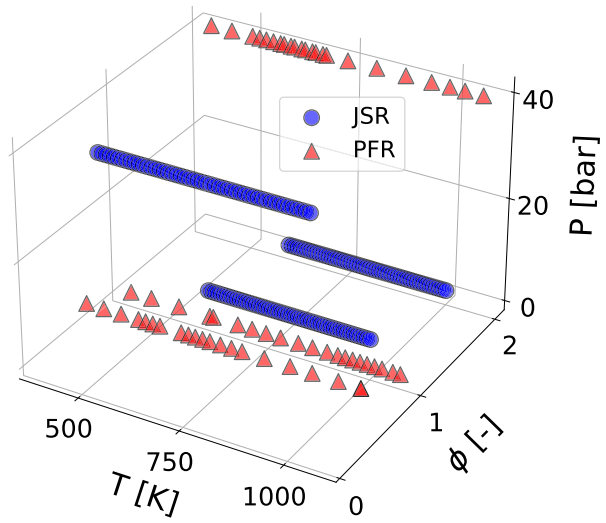

Fig. 4. Operating conditions of the artificially generated data adopted as optimization targets, represented in the space of temperature, pressure, and equivalence ratio.

can easily lead to compensations of errors in the rates. These may not raise complications in the mechanism itself but inevitably undermine the robustness of reaction-class-based mechanisms of longer fuels.

Reactions not belonging to the DMM sub-model were excluded from the optimization to preserve the mechanism consistency and to isolate the impact of the effects of lumping on the model performance. Only reactions with a relative sensitivity coefficient higher than 0.1 were optimized. This value was verified to well balance effectiveness and a limited number of parameters to optimize. An excessive number of optimization parameters leads to a slower optimization procedure and reduces the efficiency of the evolutionary algorithm in finding the optimum [43]. If all rates are optimized regardless of their impact on the complete mechanism, as previously done in the literature [32], the overall approach turns out inevitably time-consuming, and this drawback is expected to exponentially increase with the mechanism size.

The objective function was minimized using numerical data generated from the detailed model as targets. It was based on a Curve Matching algorithm [45]: after converting the model predictions of both the detailed and lumped kinetic models into functional data, the related agreement was quantified using the mean of an extended L^2-norm, as well as Pearson correlations to compare the shape of the curves and those of their first derivatives. In this way, the agreement between the predictions was quantified more comprehensively than with the typical sum of squared deviations generally used for model assessment [46]. Further numerical details about the optimization procedure and convergence criteria are available in the reference works [43–45].

The concentrations of species at the outlet of jet stirred and plug flow reactors (JSRs, PFRs) were chosen as optimization targets. Indirect properties, such as ignition delay times (IDTs) in shock tubes, were considered only for model validation. Indeed, preserving the accuracy on major species profiles and evolution over time and temperature is a necessary step to preserve accuracy on IDTs too, and allows a physically consistent optimization procedure with predictivity features. The target species were selected from the main decomposition products of alkyl radicals, hydroperoxy alkyl radicals, and keto-hydroperoxides, to account for high-, intermediate-, and low-temperature chemistry. In the DMM chemistry, these products are CH_2O and CH_3OCHO for all decompositions. Also, the fuel was chosen as a target to control its global reactivity.

Therefore, the concentrations of the fuel (DMM), CH_2O, and CH_3OCHO, as predicted by the detailed model at different temperatures in the T = 500–1100 K range, were selected as targets. The data were

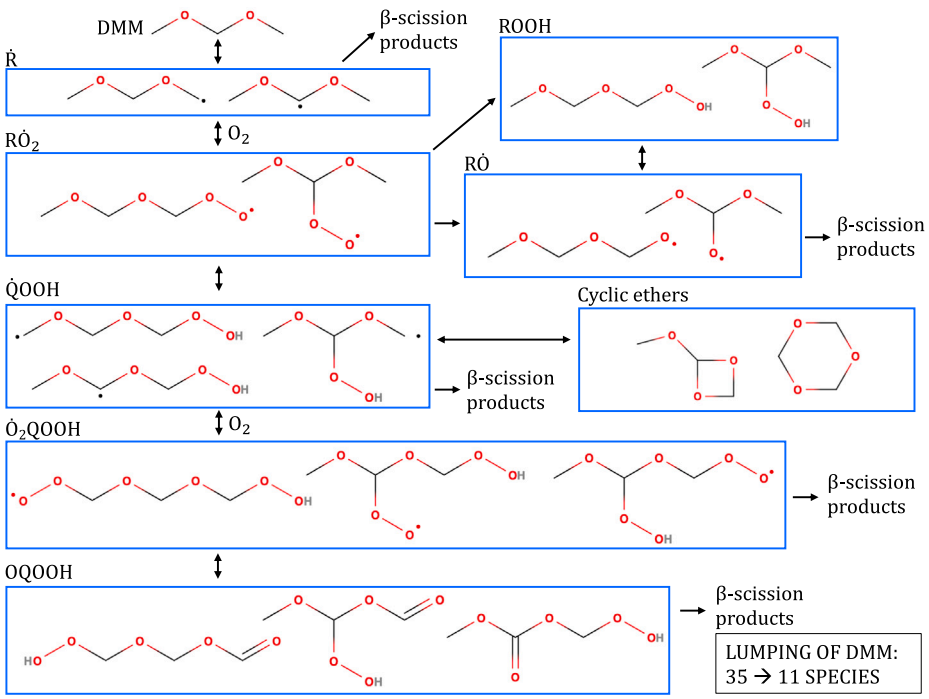

Fig. 5. Schematic representation of DMM kinetic mechanism. Blue rectangles group lumped isomers.

obtained from simulations performed at various operating conditions, sampled from a range of P = 1–40 atm (logarithmically spaced) and Φ = 0.25–2 (equispaced). In particular, the following combinations were selected, as represented in Fig. 4:

- 3 JSR simulations at: P = 1 atm and Φ = 2.0, P = 6 atm and Φ = 1.0, and P = 40 atm and Φ = 0.25;
- 3 PFR simulations at: P = 1 atm and Φ = 1.0, P = 6 atm and Φ = 0.5, and P = 40 atm and Φ = 2.0.

In such a way, the outlet concentrations of the three species were simulated at three operating conditions for 50 temperatures for JSRs, and 23, 20, and 21 temperatures for PFRs, for a total of 642 optimization targets. The choice of the operating condition was verified not to heavily influence the optimization results. The uncertainties of the target data were not considered in this optimization since they resulted from numerical simulations and are not affected by experimental uncertainty.

3. Results and discussion

3.1. Pathways identification and mechanism lumping

The lumping procedure performed on the detailed kinetic mechanism of Jacobs et al. [22] is schematized in Fig. 5. The low-temperature oxidation species can be identified, i.e., DMM alkyl (Ṙ), peroxy (RȮ$_2$), alkoxy (RȮ), hydroperoxy alkyl (Q̇OOH), and hydroperoxy alkyl peroxy (Ȯ$_2$QOOH) radicals, hydroperoxides (ROOH), keto-hydroperoxides (OQOOH), and cyclic ethers. All the pseudospecies were defined according to structural isomerism.

A limited number of species, automatically identified by MEL, were removed from the detailed mechanism to perform a preliminary reduction to simplify the mechanism and facilitate the following lumping procedure. Such species are the keto-alkyl and keto-alkoxy radicals, the alkyl ketones, the di-hydroperoxides, and the cyclic ether-hydroperoxides. After verifying that these species did not affect the mechanism performances in IDTs, speciations in JSRs and PFRs, and laminar flame speeds (LFSs), they were replaced with their decomposition products.

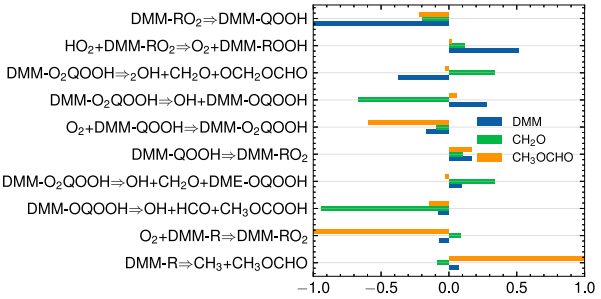

Fig. 6. 10 most sensitive DMM reactions in JSR at Φ = 0.25, P = 40 atm, and T = 600 K with their relative sensitivity coefficients. H-abstractions have already been excluded.

All the reaction pathways were lumped according to Eqs. (3) and (4), adopting the BFs calculated as in Eq. (1). The resulting lumped mechanism includes 137 species (24 less than the detailed one) and 2203 reactions, and it is available in CHEMKIN format in the SM.

3.2. Reactions selection and optimization

The selection of the reactions to be optimized was performed via a systematic calculation of the local, normalized sensitivity coefficients, throughout the whole range of operating conditions. Sensitivity analyses on DMM, CH_2O, and CH_3OCHO were performed at various temperatures and pressures in JSRs and PFRs at lean (Φ = 0.25–0.5), stoichiometric (Φ = 1.0), and rich (Φ = 2.0) conditions. The most sensitive reactions in a JSR at Φ = 0.25, P = 40 atm, and T = 600 K are reported as examples in Fig. 6 with their relative sensitivity coefficients. These conditions effectively emphasize the contributions of the low-temperature chemistry. The sensitivity analyses in PFRs highlighted the same reactions that emerged from JSRs.

The sensitivity coefficients emphasize the critical role of the decompositions of the keto-hydroperoxide and the alkyl and hydroperoxy alkyl peroxy radicals. Nevertheless, they usually have an antagonistic effect on the formation or destruction of the products i.e., improvements in one species' profile worsen the results of the other's.

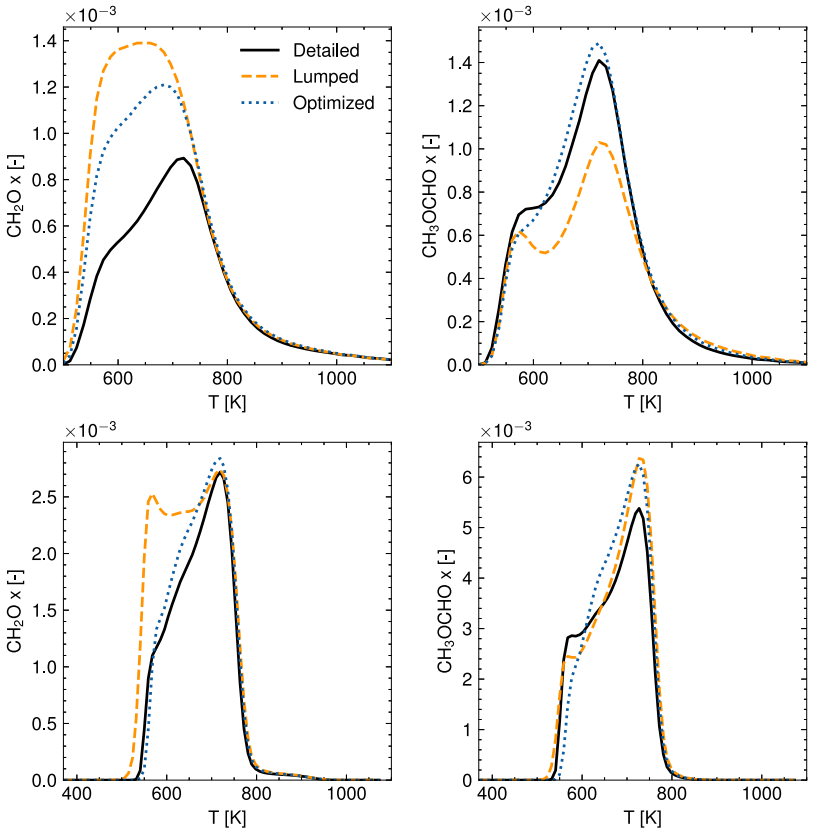

Fig. 7. An example of optimization targets before and after the optimization, compared to the detailed mechanism. The first row shows the results of a JSR simulation at $P = 40$ atm and $\Phi = 0.25$ are reported, while the second shows those from a PFR at $P = 1$ atm and $\Phi = 1.0$.

Hence their optimization inevitably met a trade-off between CH_2O and CH_3OCHO predictions. The addition of oxygen to the alkyl and hydroperoxy radicals, and its isomerization also emerged from most sensitivity analyses.

The three modified-Arrhenius parameters of 18 selected reactions (6 in PLOG format) were optimized, for a total of 54 parameters. These are reported in the SM, before and after optimization. The optimized mechanism is also available in the SM in CHEMKIN format.

The differences between the target species' predictions by the lumped and detailed mechanisms are highlighted by high-pressure and lean conditions, that promote low-temperature chemistry. Indeed, at low pressures and rich conditions, the performances of the lumped and detailed kinetic models agree even before the numerical optimization. This is exemplified in Fig. 7, where it can be noticed that species profiles improve with the optimization, but do not match the detailed ones in the critical conditions mentioned. The residual lack of agreement between detailed and optimized mechanisms must be attributed to the already cited antagonistic effect that the alkyl radicals and keto-hydroperoxides decompositions have on the formation and destruction of CH_2O and CH_3OCHO. The behavior is due to the reduced number of degrees of freedom of the lumped mechanism, and it can be partially seen in the JSR sensitivity analysis reported in Fig. 6. These discrepancies are even more evident in low-pressure PFR simulations. Nevertheless, noticeable improvements were achieved for all the target conditions. All targets are reported in the SM.

3.3. Mechanism validation

The optimized mechanism was extensively tested through a large database, covering a wide range of operating conditions and reactors. The experimental data considered are IDTs [22,47–50], LFSs [26,47], and speciations in JSRs [21,24,51,52] and PFRs [53–55]. The validation procedure was automatically performed by exploiting the novel SciExpeM platform [56,57] (available at https://sciexpem.polimi.it), which collects a large database of experiments and kinetic mechanisms, allowing to quickly simulate the data and quantify the results with the Curve Matching procedure it embeds.

The main results are reported hereafter, while the complete validation can be found in the SM, together with a comparison between this mechanism and those by Shrestha et al. [26] (37 species in the DMM sub-mechanism), Li et al. [25] (35 species), Kathrotia et al. [27] (8 species), and Sun et al. [24] (30 species). It is worth reminding that the experimental data were not optimization targets, but they are reported in the plots along with their uncertainties, to quantify the discrepancy between detailed and reduced models, in relation to the existing difference between models and experiments. For this reason, some deviations of the original detailed mechanism from the data are still present in the optimized one, but their adjustment is outside the scope of this work.

Fig. 8 compares the capability of detailed and lumped mechanisms in predicting the IDTs measured by Jacobs et al. [22] and Gillespie [47] in various conditions. The detailed mechanism reasonably predicts the ignition behaviors in all cases. The lumping procedure causes an acceleration of the mechanism predictions at low temperatures, with a maximum deviation of a factor ~1.5 from the detailed model. The predictions of the lumped mechanism thus worsened for $T < 800$ K. The optimization of the lumped model led to a substantial improvement at low temperatures while maintaining the performances of the detailed mechanism at intermediate and high temperatures.

The sensitivity coefficients for OH mass fraction (considered as representative of IDT) of the 10 most sensitive reactions in a shock tube simulation at $\Phi = 1.0$, $P = 40$ atm, and $T = 714$ K are shown in Fig. 9. The ratio between the optimized and nominal rate constant is reported for each reaction. Coherently with what is shown in Fig. 9, reactions that accelerate IDTs have their rate constants reduced with optimization, while rate constants whose reactions delay IDTs are increased.

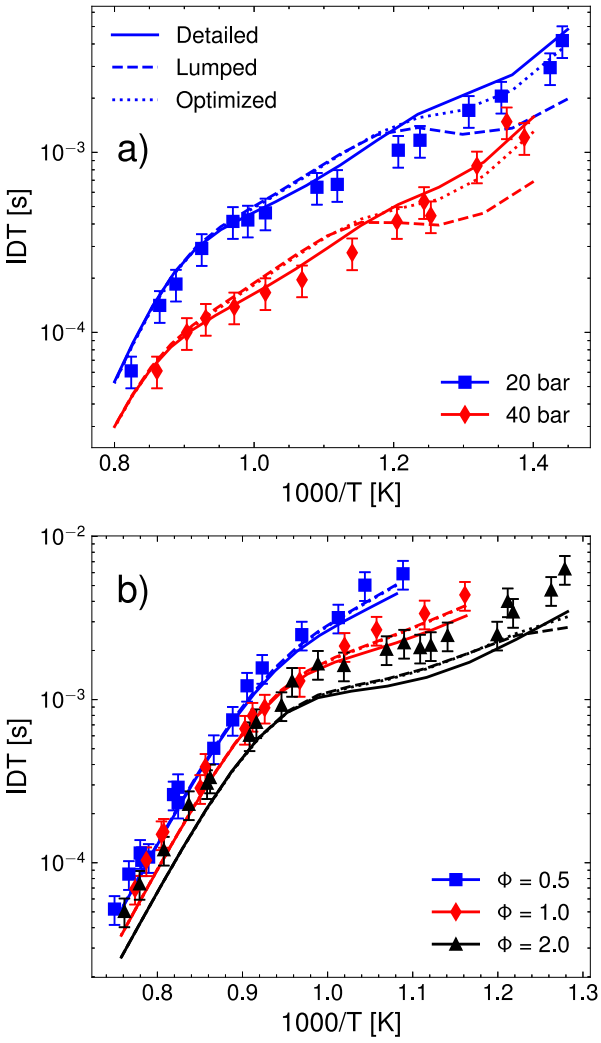

Fig. 8. DMM IDTs measured by Jacobs et al. [22] at $\Phi = 1.0$ (a) and Gillespie [47] at $P = 9$ bar (b), with relative experimental uncertainties and models predictions.

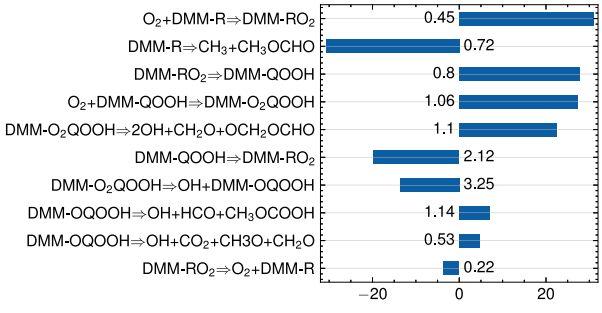

Fig. 9. Sensitivity coefficients of the 10 most sensitive reactions for OH mass fraction in a shock tube simulation at $\Phi = 1.0$, $P = 40$ atm and $T = 714$ K. For each one, the ratios between the optimized and the nominal rates are reported.

This is in agreement with the over-reactive low-temperature kinetics of the lumped model. Since IDTs were not included as optimization targets, their improvement and the consistent changes in the rates support the robustness of the proposed method.

The general validity of the mechanism is confirmed by the LFS predictions, as reported in Fig. 10 along with the measurements by Gillespie [47]. The most sensitive reactions belong to the C_0-C_3 mechanism and hence were not modified. For this reason, neither the lumping

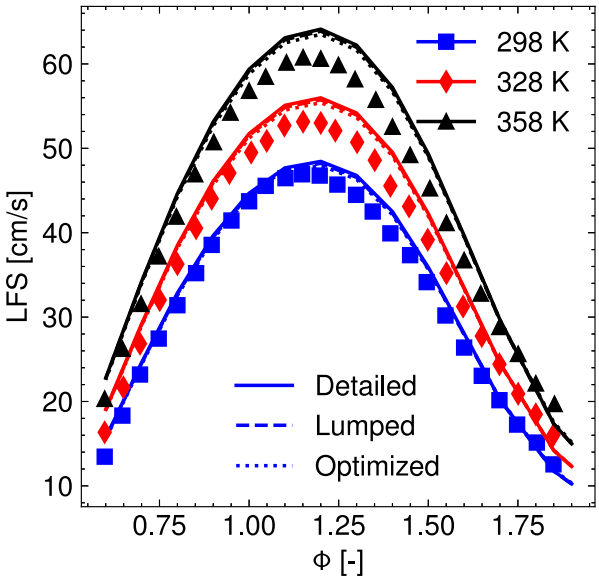

Fig. 10. LFSs measured by Gillespie [47], with relative experimental uncertainties and models predictions. DMM is diluted in air and the pressure is atmospheric.

nor the optimization procedures affected the LFS predictions, which remain as good as those of the detailed mechanism.

Species concentrations measured in a JSR by Vermeire et al. [21] ($P = 1.07$ bar, $T = 500$–1100 K, and $\Phi = 0.25$–2) are compared with the simulation results in Fig. 11. Results for $\Phi = 1$ are represented only in the range $T < 1000$ K because no steady-state solution was found for higher temperatures due to oscillating behaviors. This is suggested by the fluctuations of mole fractions regardless of the mechanism adopted (detailed, lumped, or optimized) and is due to the role of recombination reactions [58,59]. In general, mole fractions of all the species are well reproduced by all models. The detailed and lumped mechanisms over-predict the DMM reactivity for $T < 600$ K at lean conditions, but optimization corrected this error despite being in seemingly contradiction with the scope of this work. This is a consequence of the optimization of the CH_2O and CH_3OCHO profiles and suggests that this approach can correct compensations of errors present in the detailed mechanism. Indeed DMM, CH_2O, and CH_3OCHO equally contribute to the objective function, but CH_2O and CH_3OCHO could not be improved simultaneously by modifying the keto-hydroperoxide decompositions. These reactions compete for the target production and consumption, but in the lumped model there are fewer species and reactions, hence a reduced number of degrees of freedom. The only possible compromise for the optimizer was therefore to reduce the fuel reactivity, which also resulted in an improved accordance with the experimental data.

Fig. 12 collects the species concentrations measured in a PFR by Marrodán et al. [53] ($P = 20$–60 bar, $T = 800$–1100 K, and $\lambda = 0.7$). All three mechanisms at lower pressures well represent the DMM mole fraction, but the low-temperature reactivity is slightly overemphasized for $P > 40$ bar. This is especially true for the detailed mechanism but is sensibly improved with the lumping procedure. CO, CO_2, and CH_4 present discrepancies for $T > 800$ K, and CH_3OCHO behavior is not well reproduced for lower pressures. CH_2O, contrary to the JSR simulations, is under-predicted by the detailed model too, and its improvement was antagonistic with the behavior of other species, mainly CH_3OCHO. In this specific case, the optimized mechanism does not differ significantly from the lumped one. The improved agreement with the experimental data of the DMM conversion, despite the discrepancies with the detailed mechanism, is justified again by the contributions of CH_2O and CH_3OCHO to the objective function.

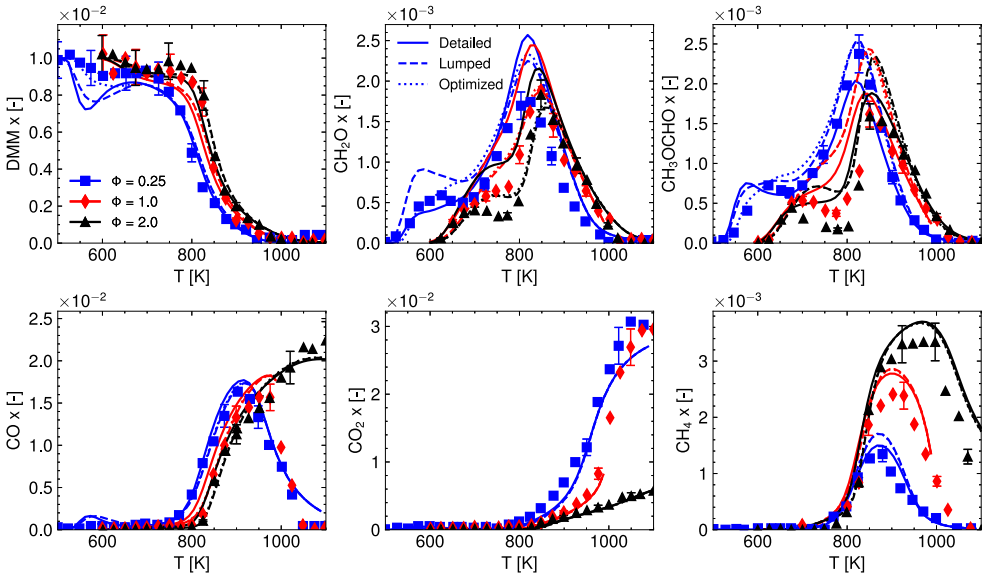

Fig. 11. Species mole fractions of DMM combustion products measured in a JSR by Vermeire et al. [21], with relative experimental uncertainties and model predictions (P = 1.07 bar, T = 500–1100 K, and Φ = 0.25–2; DMM diluted in 99% O_2 and Ar). Additional species profiles and pyrolysis conditions are shown in the SM.

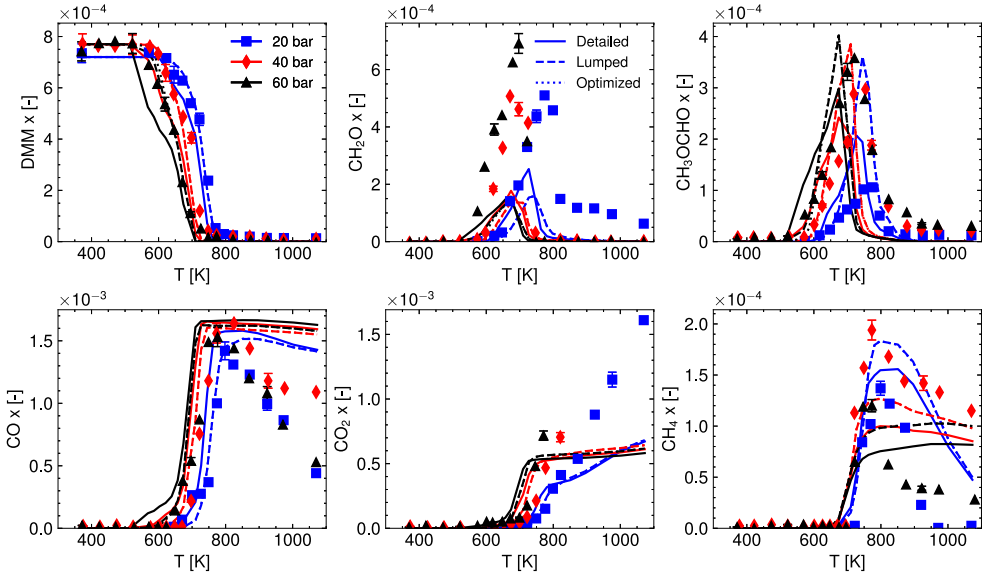

Fig. 12. Species mole fractions of DMM combustion products measured in a PFR by Marrodán et al. [53], with relative experimental uncertainties and model predictions. DMM and O_2 are diluted in N_2. Experiments are carried out at P = 20–60 bar and λ = 0.7. In this case, the results of the lumped and optimized mechanisms do not differ significantly from each other. Results for leaner mixtures can be found in the SM.

A comprehensive evaluation of the mechanism performance is extensively provided in Section 1 of SM. Results are quantitatively summarized in the heatmap in Fig. 13 in terms of the average Curve Matching scores [45] for each mechanism. The experiments are identified by their ID numbers on SciExpeM. As described in the reference work [45], such a framework allows a standardized evaluation of the model-experiments agreement, providing a quantitative score for each comparison, bounded between 0 (maximum disagreement) and 1 (perfect agreement). Curve Matching scores for PFR and JSR simulations are averaged among all the species investigated.

The optimized mechanism, compared to the performances of the starting mechanism, exhibits similar scores for the whole range of conditions. In most conditions where a worsening of the lumped model performance is seen, the optimization proved effective in recovering the original behavior. LFSs were mostly uninfluenced by both lumping and optimization, as expected. The worse predictions obtained for the Shrestha et al. [26] measurements suggest that the mechanism could be refined by optimizing it with LFSs as experimental targets.

Finally, to demonstrate the generality of the approach, the same lumping-optimization procedure has been applied to a detailed mechanism of OME_2, built from the sub-mechanism of Cai et al. [60]. The number of species in the sub-mechanism was automatically reduced from 29 to 10. The validation of the mechanism is available in the SM and confirms that the methodology is solid and can be adopted to reduce more complex fuels.

4. Conclusions

In this work, an automatic and integrated methodology coupling the lumping of isomers and a data-driven optimization approach exploiting artificial data generation was presented and applied to the kinetic modeling of DMM as a case study. To this purpose, a detailed mechanism

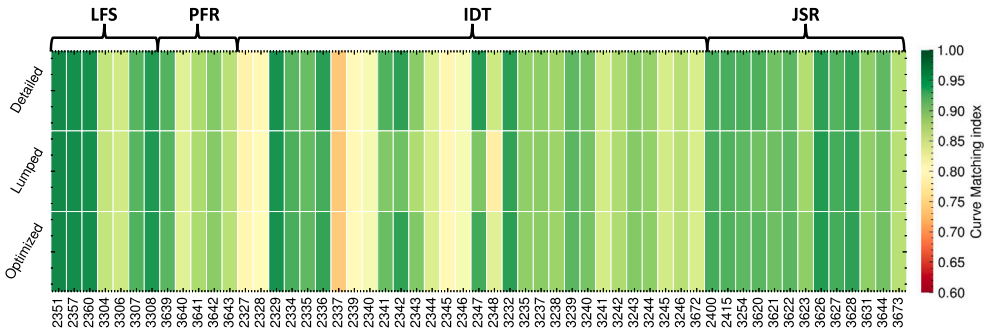

Fig. 13. Curve Matching scores for DMM experimental datasets, evaluated for the three mechanisms. Values on the *x*-axis are the ID number of the experiments on SciExpeM.

was first built in a modular way, starting from a consolidated C_0-C_3 core mechanism, then hierarchically adding literature sub-mechanisms for DME [36] and DMM [22]. As a second step, a lumping methodology based on the grouping of structural isomers was applied, allowing the reduction of the mechanism from 35 to 11 species. Finally, the lumped mechanism underwent an optimization procedure [43] based on an evolutionary algorithm, targeting the speciation predictions of the detailed mechanism in different operating conditions. 16 reactions of the DMM sub-mechanism were optimized using an objective function based on the Curve Matching parameter [45]. This also allowed a comprehensive quantification of the agreement between the experimental profiles and the modeling predictions. The optimized mechanism was automatically validated through a large database, exploiting the SciExpeM platform [56,57]. Its qualitative and quantitative assessment confirmed that its predictive capability in the investigated experimental datasets is comparable to the starting detailed mechanism. Even indirect properties, such as IDTs, improved despite the optimization being performed using only species concentrations as targets. The sensitivity analyses subsequently performed at the conditions where IDTs improved, confirmed that the optimized reactions were indeed the controlling ones in the investigated conditions, supporting the coherence of the proposed method. The good agreement with the original model was also confirmed in 1D flames, where reactivity is driven by reactions belonging to the C_0-C_3 core mechanism, not involved in the optimization procedure [33]. This paves the way to Computational Fluid Dynamics (CFD) applications of such a mechanism, which have not been investigated in this work for the sake of compactness, though.

The lumping procedure proposed, besides the selection of the pseudospecies and the calculation of their BFs, is fully automatic. It indeed provides temperature- and pressure-dependent rate constants after performing a small set of simulations that are independent from the validation datasets [40]. While human intervention is still required, the level of automation is very high. Additionally, this work is one of the first cases of application to a large set of reactions involving different stoichiometries. This greatly increases the level of complexity compared to standard MEL applications, thus the need to couple it with the optimization procedure. In turn, the computational time for model optimization was significantly reduced thanks to the previous lumping.

This successful application of the lumping-optimization coupling on DMM chemistry is also promising for longer-chain fuels. Nevertheless, there is still room for improvement for more systematic and efficient hierarchical modeling. Future research will involve the implementation of methodologies for hierarchical lumping and optimization procedures based on reaction classes, as already done in the literature [29,61] but never integrated into a single framework. This methodology will find an immediate application in the longer-chain OMEs, of which DMM is the archetypal species, where the extent of the reduction is expected to be more significant.

Novelty and significance statement

This work presents an automatic lumping methodology to reduce detailed mechanisms by grouping isomers into pseudospecies, and by determining their lumped reactivity through their composition. Such a procedure has been synergistically coupled to a data-driven optimization of the most sensitive reaction rates, whose consistency is ensured by physically-sound boundaries, based on artificial data generation. The result is a novel and automatic approach to obtain, starting from an available detailed kinetic mechanism, a lumped one whose chemistry is consistent with the low-, medium-, and high-temperature reactivity of the fuel. The resulting lumped mechanism is suitable for further reduction (e.g., up to a skeletal level) to derive a kinetic model appropriate for computational fluid dynamics simulations. The procedure is not fuel-specific but relies instead on general concepts and it can hence be applied to other novel fuels of interest, aiding the modeling community to speed up the predictions of combustion models, key for emissions reduction or alternative fuels investigation.

CRediT authorship contribution statement

Alessandro Pegurri: Methodology, Conducted the procedures, Writing – original draft. **Timoteo Dinelli:** Definition of the optimization methodology, Writing – review & editing. **Luna Pratali Maffei:** Definition of the lumping procedure, Writing – review & editing. **Tiziano Faravelli:** Definition of the methodology, Writing – review & editing. **Alessandro Stagni:** Supervised the definition of the methodology, Writing – review & editing.

Declaration of competing interest

The authors declare that they have no known competing financial interests or personal relationships that could have appeared to influence the work reported in this paper.

Acknowledgments

Luna Pratali Maffei's contribution to this study was carried out within the NEST - Network 4 Energy Sustainable Transition (D.D. 1243 02/08/2022, PE00000021) and received funding under the National Recovery and Resilience Plan (NRRP), Mission 4 Component 2 Investment 1.3, funded by the European Union - NextGenerationEU. This manuscript reflects only the author's views and opinions, neither the European Union nor the European Commission can be considered responsible for them.

Supplementary materials

Supplementary material related to this article can be found online at https://doi.org/10.1016/j.combustflame.2023.113202.

References

[1] M. Eurostat, Energy, transport and environment statistics, 2019.
[2] R. Plan, Communication from the Commission to the European Parliament, the European Council, the Council, the European Economic and Social Committee and the Committee of the Regions, European Commission: Brussels, Belgium, 2018.
[3] A. Ramirez, S.M. Sarathy, J. Gascon, CO_2 derived E-fuels: research trends, misconceptions, and future directions, Trends Chem. 2 (9) (2020) 785–795.
[4] K. Kohse-Höinghaus, Combustion in the future: The importance of chemistry, Proc. Combust. Inst. 38 (1) (2021) 1–56.
[5] K. Thenert, K. Beydoun, J. iesenthal, W. Leitner, n. Jürgen Klankermayer, K. Thenert, J. Wiesenthal, D. Leitner, D.L. eitner, Ruthenium-catalyzed synthesis of dialkoxymethane ethers utilizing carbon dioxide and molecular hydrogen, Angew. Chem. 128 (40) (2016) 12454–12457.
[6] B.G. Schieweck, J. Klankermayer, Tailor-made molecular cobalt catalyst system for the selective transformation of carbon dioxide to dialkoxymethane ethers, Angew. Chem. Int. Ed. 56 (36) (2017) 10854–10857.
[7] S. Deutz, D. Bongartz, B. Heuser, A. Kätelhön, L. Schulze Langenhorst, A. Omari, M. Walters, J. Klankermayer, W. Leitner, A. Mitsos, S. Pischinger, A. Bardow, Cleaner production of cleaner fuels: wind-to-wheel – environmental assessment of CO 2 -based oxymethylene ether as a drop-in fuel, Energy Environ. Sci. 11 (2) (2018) 331–343.
[8] D. Bongartz, J. Burre, A. Mitsos, Production of oxymethylene dimethyl ethers from hydrogen and carbon dioxide - part I: Modeling and analysis for OME1, Ind. Eng. Chem. Res. 58 (12) (2019) 4881–4889.
[9] M. Härtl, K. Gaukel, D. Pélerin, G. Wachtmeister, Oxymethylene ether as potentially CO2-neutral fuel for clean diesel engines part 1: Engine testing, MTZ worldwide 78 (2) (2017) 52–59.
[10] M.B. Sirman, E.C. Owens, K.A. Whitney, Emissions comparison of alternative fuels in an advanced automotive diesel engine, SAE Trans. (2000) 2166–2176.
[11] R. Zhu, H. Miao, X. Wang, Z. Huang, Effects of fuel constituents and injection timing on combustion and emission characteristics of a compression-ignition engine fueled with diesel-DMM blends, Proc. Combust. Inst. 34 (2) (2013) 3013–3020.
[12] A. Omari, B. Heuser, S. Pischinger, C. Rüdinger, Potential of long-chain oxymethylene ether and oxymethylene ether-diesel blends for ultra-low emission engines, Appl. Energy 239 (2019) 1242–1249.
[13] J. Liu, H. Wang, Y. Li, Z. Zheng, Z. Xue, H. Shang, M. Yao, Effects of diesel/PODE (polyoxymethylene dimethyl ethers) blends on combustion and emission characteristics in a heavy duty diesel engine, Fuel 177 (2016) 206–216.
[14] Y.R. Tan, M. Salamanca, L. Pascazio, J. Akroyd, M. Kraft, The effect of poly (oxymethylene) dimethyl ethers (PODE3) on soot formation in ethylene/PODE3 laminar coflow diffusion flames, Fuel 283 (2021) 118769.
[15] H. Zhang, D. Kaczmarek, C. Rudolph, S. Schmitt, N. Gaiser, P. Oßwald, T. Bierkandt, T. Kasper, B. Atakan, K. Kohse-Höinghaus, Dimethyl ether (DME) and dimethoxymethane (DMM) as reaction enhancers for methane: Combining flame experiments with model-assisted exploration of a polygeneration process, Combust. Flame 237 (2022) 111863.
[16] D. Goeb, M. Davidovic, L. Cai, P. Pancharia, M. Bode, S. Jacobs, J. Beeckmann, W. Willems, K.A. Heufer, H. Pitsch, Oxymethylene ether–n-dodecane blend spray combustion: Experimental study and large-eddy simulations, Proc. Combust. Inst. 38 (2) (2021) 3417–3425.
[17] R. Novella, G. Bracho, J. Gomez-Soriano, C.S. Fernandes, T. Lucchini, Combustion system optimization for the integration of e-fuels (Oxymethylene Ether) in compression ignition engines, Fuel 305 (2021) 121580.
[18] F. Ferraro, C. Russo, R. Schmitz, C. Hasse, M. Sirignano, Experimental and numerical study on the effect of oxymethylene ether-3 (OME3) on soot particle formation, Fuel 286 (2021) 119353.
[19] R. Schmitz, M. Sirignano, C. Hasse, F. Ferraro, Numerical investigation on the effect of the oxymethylene ether-3 (OME3) blending ratio in premixed sooting ethylene flames, Front. Mech. Eng. 7 (2021) 744172.
[20] R. Schmitz, F. Ferraro, M. Sirignano, C. Hasse, Numerical and experimental investigations on the particle formation in oxymethylene ethers (OMEn, n=2-4)/ethylene premixed flames, Fuel 357 (2024) 129762.
[21] F.H. Vermeire, H.-H. Carstensen, O. Herbinet, F. Battin-Leclerc, G.B. Marin, K.M. Van Geem, Experimental and modeling study of the pyrolysis and combustion of dimethoxymethane, Combust. Flame 190 (2018) 270–283.
[22] S. Jacobs, M. Döntgen, A.B. Alquaity, W.A. Kopp, L.C. Kröger, U. Burke, H. Pitsch, K. Leonhard, H.J. Curran, K.A. Heufer, Detailed kinetic modeling of dimethoxymethane. Part II: Experimental and theoretical study of the kinetics and reaction mechanism, Combust. Flame 205 (2019) 522–533.
[23] T. He, H.-y. Liu, Y. Wang, B. Wang, H. Liu, Z. Wang, Development of surrogate model for oxygenated wide-distillation fuel with polyoxymethylene dimethyl ether, SAE Int. J. Fuels Lubr. 10 (3) (2017) 803–814.
[24] W. Sun, T. Tao, M. Lailliau, N. Hansen, B. Yang, P. Dagaut, Exploration of the oxidation chemistry of dimethoxymethane: Jet-stirred reactor experiments and kinetic modeling, Combust. Flame 193 (2018) 491–501.
[25] N. Li, W. Sun, S. Liu, X. Qin, Y. Zhao, Y. Wei, Y. Zhang, A comprehensive experimental and kinetic modeling study of dimethoxymethane combustion, Combust. Flame 233 (2021) 111583.
[26] K.P. Shrestha, S. Eckart, A.M. Elbaz, B.R. Giri, C. Fritsche, L. Seidel, W.L. Roberts, H. Krause, F. Mauss, A comprehensive kinetic model for dimethyl ether and dimethoxymethane oxidation and NOx interaction utilizing experimental laminar flame speed measurements at elevated pressure and temperature, Combust. Flame 218 (2020) 57–74.
[27] T. Kathrotia, P. Oßwald, C. Naumann, S. Richter, M. Köhler, Combustion kinetics of alternative jet fuels, part-II: Reaction model for fuel surrogate, Fuel 302 (2021) 120736.
[28] T. Lu, C.K. Law, Toward accommodating realistic fuel chemistry in large-scale computations, Prog. Energy Combust. Sci. 35 (2) (2009) 192–215.
[29] E. Ranzi, A. Frassoldati, S. Granata, T. Faravelli, Wide-range kinetic modeling study of the pyrolysis, partial oxidation, and combustion of heavy n-alkanes, Ind. Eng. Chem. Res. 44 (14) (2005) 5170–5183.
[30] S.S. Ahmed, F. Mauß, G. Moréac, T. Zeuch, A comprehensive and compact n-heptane oxidation model derived using chemical lumping, Phys. Chem. Chem. Phys. 9 (9) (2007) 1107–1126.
[31] A. Stagni, A. Cuoci, A. Frassoldati, T. Faravelli, E. Ranzi, Lumping and reduction of detailed kinetic schemes: an effective coupling, Ind. Eng. Chem. Res. 53 (22) (2014) 9004–9016.
[32] P. Pepiot-Desjardins, H. Pitsch, An automatic chemical lumping method for the reduction of large chemical kinetic mechanisms, Combust. Theory Model. 12 (6) (2008) 1089–1108.
[33] E. Ranzi, A. Frassoldati, R. Grana, A. Cuoci, T. Faravelli, A.P. Kelley, C.K. Law, Hierarchical and comparative kinetic modeling of laminar flame speeds of hydrocarbon and oxygenated fuels, Prog. Energy Combust. Sci. 38 (4) (2012) 468–501.
[34] W.K. Metcalfe, S.M. Burke, S.S. Ahmed, H.J. Curran, A hierarchical and comparative kinetic modeling study of C_1-C_2 hydrocarbon and oxygenated fuels, Int. J. Chem. Kinet. 45 (10) (2013) 638–675.
[35] G. Bagheri, E. Ranzi, M. Pelucchi, A. Parente, A. Frassoldati, T. Faravelli, Comprehensive kinetic study of combustion technologies for low environmental impact: MILD and OXY-fuel combustion of methane, Combust. Flame 212 (2020) 142–155.
[36] S.M. Burke, U. Burke, R. Mc Donagh, O. Mathieu, I. Osorio, C. Keesee, A. Morones, E.L. Petersen, W. Wang, T.A. DeVerter, et al., An experimental and modeling study of propene oxidation. Part 2: Ignition delay time and flame speed measurements, Combust. Flame 162 (2) (2015) 296–314.
[37] E. Ranzi, M. Dente, T. Faravelli, G. Pennati, Prediction of kinetic parameters for hydrogen abstraction reactions, Combust. Sci. Technol. 95 (1–6) (1993) 1–50.
[38] U. Burke, K.P. Somers, P. O'Toole, C.M. Zinner, N. Marquet, G. Bourque, E.L. Petersen, W.K. Metcalfe, Z. Serinyel, H.J. Curran, An ignition delay and kinetic modeling study of methane, dimethyl ether, and their mixtures at high pressures, Combust. Flame 162 (2) (2015) 315–330.
[39] B. Ruscic, D. Bross, Active Thermochemical Tables (ATcT) values based on ver. 1.122 d of the Thermochemical, Network (2018).
[40] L.P. Maffei, M. Pelucchi, C. Cavallotti, A. Bertolino, T. Faravelli, Master equation lumping for multi-well potential energy surfaces: a bridge between ab initio based rate constant calculations and large kinetic mechanisms, Chem. Eng. J. 422 (2021) 129954.
[41] A. Stagni, A. Frassoldati, A. Cuoci, T. Faravelli, E. Ranzi, Skeletal mechanism reduction through species-targeted sensitivity analysis, Combust. Flame 163 (2016) 382–393.
[42] L. Heberle, P. Pepiot, Automatic identification and lumping of high-temperature fuel decomposition pathways for chemical kinetics mechanism reduction, Proc. Combust. Inst. 38 (1) (2021) 1053–1061.
[43] A. Bertolino, M. Fürst, A. Stagni, A. Frassoldati, M. Pelucchi, C. Cavallotti, T. Faravelli, A. Parente, An evolutionary, data-driven approach for mechanism optimization: theory and application to ammonia combustion, Combust. Flame 229 (2021) 111366.
[44] M. Fürst, A. Bertolino, A. Cuoci, T. Faravelli, A. Frassoldati, A. Parente, OptiSMOKE++: A toolbox for optimization of chemical kinetic mechanisms, Comput. Phys. Comm. 264 (2021) 107940.
[45] M. Pelucchi, A. Stagni, T. Faravelli, Addressing the complexity of combustion kinetics: Data management and automatic model validation, in: Computer Aided Chemical Engineering, Vol. 45, Elsevier, 2019, pp. 763–798.
[46] C.J. Willmott, On the validation of models, Phys. Geogr. 2 (2) (1981) 184–194.
[47] F.R. Gillespie, An Experimental and Modelling Study of the Combustion of Oxygenated Hydrocarbons, National University of Ireland, 2014.
[48] E. Hu, Z. Gao, Y. Liu, G. Yin, Z. Huang, Experimental and modeling study on ignition delay times of dimethoxy methane/n-heptane blends, Fuel 189 (2017) 350–357.
[49] J. Herzler, M. Fikri, C. Schulz, High-pressure shock-tube study of the ignition and product formation of fuel-rich dimethoxymethane (DMM)/air and CH4/DMM/air mixtures, Combust. Flame 216 (2020) 293–299.
[50] C. Zhang, P. Li, Y. Li, J. He, X. Li, Shock-tube study of dimethoxymethane ignition at high temperatures, Energy & Fuels 28 (7) (2014) 4603–4610.
[51] C.A. Daly, J.M. Simmie, P. Dagaut, M. Cathonnet, Oxidation of dimethoxymethane in a jet-stirred reactor, Combust. Flame 125 (3) (2001) 1106–1117.

[52] Z. Gao, E. Hu, Z. Xu, G. Yin, Z. Huang, Low to intermediate temperature oxidation studies of dimethoxymethane/n-heptane blends in a jet-stirred reactor, Combust. Flame 207 (2019) 20–35.
[53] L. Marrodan, A.J. Arnal, A. Millera, R. Bilbao, M.U. Alzueta, The inhibiting effect of NO addition on dimethyl ether high-pressure oxidation, Combust. Flame 197 (2018) 1–10.
[54] H. Zhang, S. Schmitt, L. Ruwe, K. Kohse-Höinghaus, Inhibiting and promoting effects of NO on dimethyl ether and dimethoxymethane oxidation in a plug-flow reactor, Combust. Flame 224 (2021) 94–107.
[55] L. Marrodán, F. Monge, Á. Millera, R. Bilbao, M.U. Alzueta, Dimethoxymethane oxidation in a flow reactor, Combust. Sci. Technol. 188 (4–5) (2016) 719–729.
[56] E. Ramalli, G. Scalia, B. Pernici, A. Stagni, A. Cuoci, T. Faravelli, Data ecosystems for scientific experiments: managing combustion experiments and simulation analyses in chemical engineering, Front. Big Data 4 (2021) 663410.
[57] E. Ramalli, T. Dinelli, A. Nobili, A. Stagni, B. Pernici, T. Faravelli, Automatic validation and analysis of predictive models by means of big data and data science, Chem. Eng. J. 454 (2023) 140149.
[58] A. Stagni, Y. Song, L.A. Vandewalle, K.M. Van Geem, G.B. Marin, O. Herbinet, F. Battin-Leclerc, T. Faravelli, The role of chemistry in the oscillating combustion of hydrocarbons: An experimental and theoretical study, Chem. Eng. J. 385 (2020) 123401.
[59] M. Lubrano Lavadera, Y. Song, P. Sabia, O. Herbinet, M. Pelucchi, A. Stagni, T. Faravelli, F. Battin-Leclerc, M. De Joannon, Oscillatory behavior in methane combustion: influence of the operating parameters, Energy & Fuels 32 (10) (2018) 10088–10099.
[60] L. Cai, S. Jacobs, R. Langer, F. vom Lehn, K.A. Heufer, H. Pitsch, Auto-ignition of oxymethylene ethers (OMEn, n=2–4) as promising synthetic e-fuels from renewable electricity: shock tube experiments and automatic mechanism generation, Fuel 264 (2020) 116711.
[61] L. Cai, H. Pitsch, Mechanism optimization based on reaction rate rules, Combust. Flame 161 (2) (2014) 405–415.